European Journal of Pharmaceutical Sciences 42 (2011) 199–209

Contents lists available at ScienceDirect

European Journal of Pharmaceutical Sciences

journal homepage: www.elsevier.com/locate/ejps

Flowability of surface modified pharmaceutical granules: A comparative experimental and numerical study

Ann-Sofie Persson, Göran Alderborn, Göran Frenning*

Uppsala University, Department of Pharmacy, Uppsala Biomedical Centre, P.O. Box 580, SE-751 23 Uppsala, Sweden

ARTICLE INFO

Article history:
Received 9 July 2010
Received in revised form
17 November 2010
Accepted 19 November 2010
Available online 26 November 2010

Keywords:
Discharge rate
Angle of repose
Discrete element method
Rolling and sliding friction
Cohesion

ABSTRACT

Flowability – as measured by hopper discharge rate, angle of repose and Carr's index (CI) – of surface modified microcrystalline cellulose granules was investigated experimentally. Three-dimensional simulations of the granule flow were performed, using the discrete element method (DEM), including either sliding and rolling friction or sliding friction and cohesion in the model. Granule surface modification with polymer coating and lubrication was found to have a significant effect on the sliding friction coefficient. This effect was also reflected in the ensuing flow behaviour, as quantified by the experimental discharge rate and angle of repose, whereas the results for the CI were inconclusive. The numerical results demonstrated that granular flow was qualitatively different for non-cohesive and cohesive granules, occurring in the form of individual particles for the former and in larger clusters for the latter. Rolling friction and cohesion nevertheless affected the simulated discharge rate in a similar manner, producing results comparable to those observed experimentally and calculated with the Beverloo equation. The numerical results for the cohesive granules demonstrated that cohesion alone was sufficient to produce stable heaps. However, the agreement with experimental data was satisfactory only for the non-cohesive granules, demonstrating the importance of rolling friction.

1. Introduction

Interparticle forces have a decisive influence on powder flowability (Tykhoniuk et al., 2007). Small forces (relative to gravity) offer less resistance to flow and are most often dominating in systems comprising coarse spherical particles. In pharmaceutics, free flowing powders are rare and granulation is often required to impart the desired properties. Characterization of flowability can easily be performed by determining the hopper discharge rate (Nedderman et al., 1982) and angle of repose (Train, 1958). Such methods are simple but commonly used in industry and have compendial status (European Pharmacopoeia 7th ed., 2010).

Numerical simulation has lately gained much attention for describing various powder processes. The discrete element method (DEM), originally developed by Cundall and Strack (1979), enables simulations at the particulate level, where particle positions and velocities are traced. The DEM has been used to study both hopper discharge and angle of repose.

From a practical point of view, hopper discharge is typically well-described by the Beverloo equation, which relates the discharge rate to the effective orifice diameter (excluding dead space) to the power of 5/2 (Beverloo et al., 1961). From a more theoretical point of view, a number of studies have demonstrated the ability of the DEM to predict hopper discharge rate, both for spherical (Anand et al., 2008; Datta et al., 2008; Anand et al., 2009) and non-spherical particles (Cleary and Sawley, 2002; Tao et al., 2010). Often 2D (Datta et al., 2008) or quasi-3D (Anand et al., 2008, 2009) systems have been investigated (the latter employing periodic boundary conditions in one spatial direction), but examples of fully-3D simulations exist, especially for non-spherical particles (Cleary and Sawley, 2002; Tao et al., 2010). The studies demonstrated the dependence of discharge rate on hopper angle (Datta et al., 2008) and particle–particle interactions (Anand et al., 2008), including cohesion (Anand et al., 2009). When the DEM is used, friction is typically accounted for by using effective sliding (and rolling) friction coefficients, a practice that we will adhere to. It is to be noted, however, that stick–slip phenomena may occur when surfaces slide against each other, necessitating a distinction between static and kinetic friction (Bowden and Tabor, 2001).

Although large-scale simulations encompassing up to four million particles have recently been described (Bierwisch et al., 2009), numerical studies of the angle of repose have typically focused on small systems, comprising a few thousand particles, to save computational time (Zhou et al., 1999, 2001, 2002; Li et al., 2005). Independent of the size of the simulated system, the importance of frictional forces for accurate prediction of the angle of repose

* Corresponding author. Tel.: +46 18 471 43 75; fax: +46 18 471 42 23.
E-mail address: Goran.Frenning@farmaci.uu.se (G. Frenning).

0928-0987/$ – see front matter © 2010 Elsevier B.V. All rights reserved.
doi:10.1016/j.ejps.2010.11.011

has been demonstrated. Both the sliding (Zhou et al., 2002; Li et al., 2005) and rolling friction coefficients (Zhou et al., 1999, 2001, 2002; Bierwisch et al., 2009) significantly affect heap formation and stability. Large friction coefficients decrease the kinetic energy of the particles, thereby prohibiting their translational and rotational motion. Rolling friction is mostly related to particle shape, but a dependence on surface quality and texture exists, as for the sliding friction coefficient. Inclusion of both sliding and rolling friction in the DEM model is essential for accurate prediction of the angle of repose (Zhou et al., 2001, 2002), at least for non-cohesive particles. Whereas 2D or quasi-3D simulations provide adequate predictions of hopper discharge rate, the angle of repose typically exhibits a pronounced dependence on container thickness (Zhou et al., 2001, 2002), indicating that fully-3D simulations may be required for realistic results.

Successful comparative studies between experiments and simulations of powder flowability were previously conducted for various materials (Zhou et al., 2002; Li et al., 2005; Datta et al., 2008; Bierwisch et al., 2009). The studies most frequently focused on coarse glass beads and metal powders, whereas pharmaceutical materials received little attention. However, related processes have been investigated by researchers in the pharmaceutical field, in particular particle packing and die filling (Siiriä and Yliruusi, 2007; Wu, 2008).

The main objective of this work was to appraise the capability of DEM to predict flowability for a pharmaceutically relevant yet relatively simple model material, granulated microcrystalline cellulose (MCC). The granule surfaces – and hence the interparticle forces – were modified by tacky polymer films (Chalykh et al., 2002) and by lubrication. A standard flow testing instrument was used to determine the discharge rate and angle of repose in a combined experiment. These two measures of flowability were extracted from analogous simulations, with the geometry and number of particles chosen to match the experimental work, resulting in fully-3D simulations of an intermediate sized system. A parametric study was performed to further asses the influence of sliding/rolling friction and cohesion on the discharge rate and angle of repose and to see whether cohesion alone may have a similar stabilizing effect on heaps as rolling friction.

2. Discrete element model

For simplicity, a linear cohesive model of the type described by Asmar et al. (2002) was used in the simulations. Rolling torques were included, as suggested by Zhou et al. (1999).

2.1. Kinematics

Assuming spherical particles, each particle i is characterized by its radius (R_i), mass (M_i), centre-of-mass position ($\mathbf{x}_i$), linear velocity ($\mathbf{v}_i$), and angular velocity ($\boldsymbol{\omega}_i$). Focusing on contact between two particles 1 and 2 (Fig. 1), the relative position vector $\mathbf{x}_{12} = \mathbf{x}_1 - \mathbf{x}_2$ is used to determine particle normals ($\hat{\mathbf{n}}_i$) as

$$\hat{\mathbf{n}}_1 = -\hat{\mathbf{n}}_2 = -\frac{\mathbf{x}_{12}}{|\mathbf{x}_{12}|}. \tag{1}$$

The radii vectors $\mathbf{r}_i = R_i\hat{\mathbf{n}}_i$ ($i = 1, 2$) enable the surface velocity of the particles at the contact point ($\mathbf{v}_i^s$) to be determined as

$$\mathbf{v}_i^s = \mathbf{v}_i + \boldsymbol{\omega}_i \times \mathbf{r}_i \quad (i = 1,\ 2). \tag{2}$$

Relative velocities are introduced as $\mathbf{v}_{12} = \mathbf{v}_1 - \mathbf{v}_2$ and $\mathbf{v}_{12}^s = \mathbf{v}_1^s - \mathbf{v}_2^s$, and the relative surface velocity is decomposed into normal and tangential components, $\mathbf{v}_{12}^{sn} = (\mathbf{v}_{12}^s \cdot \hat{\mathbf{n}}_1)\hat{\mathbf{n}}_1$ and $\mathbf{v}_{12}^{st} = \mathbf{v}_{12}^s - \mathbf{v}_{12}^{sn}$, respectively. Elastic contact forces are determined from the normal and tangential overlaps, which are defined as $\delta_n = R_1 + R_2 - |\mathbf{x}_{12}|$ and $\delta_t = |\mathbf{u}_{12}|$. Here, $\mathbf{u}_{12}$ is the tangential displacement of particle 1 relative to particle 2, initialized as zero when the particles first touch and during the lifetime of the contact updated via

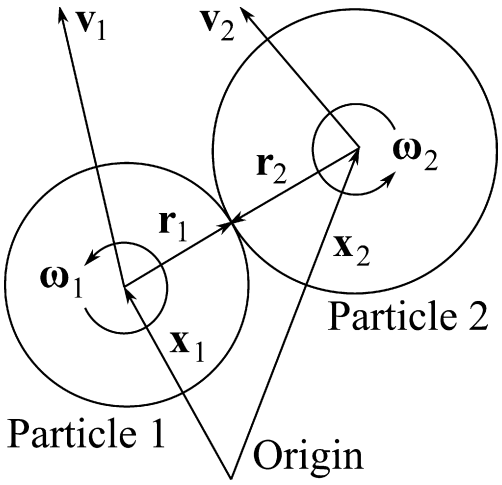

Fig. 1. Contact between two spherical particles.

$$\dot{\mathbf{u}}_{12} = s\mathbf{v}_{12}^{st} + \frac{(\mathbf{u}_{12} \cdot \mathbf{v}_{12})}{|\mathbf{x}_{12}|}\hat{\mathbf{n}}_1, \tag{3}$$

where $s = 1$ for stick and $s = 0$ for slip (see below) and the superposed dot denotes the time derivative. The second term in Eq. (3) takes into account changes in $\mathbf{u}_{12}$ that occur when both particle rotate around a common axis (Luding, 2008). Based on the tangential relative displacement, tangential unit vectors ($\hat{\mathbf{t}}_i$) are introduced as

$$\hat{\mathbf{t}}_1 = -\hat{\mathbf{t}}_2 = \frac{\mathbf{u}_{12}}{|\mathbf{u}_{12}|}. \tag{4}$$

Note that the sign conventions used in Eqs. (1) and (4) are such that repulsive normal and frictional tangential forces on particle 1 are directed along the *negative* $\hat{\mathbf{n}}_1$ and $\hat{\mathbf{t}}_1$ directions.

2.2. Forces

The force $\mathbf{F}_{12}$ on particle 1 caused by particle 2 may generally be expressed as

$$\mathbf{F}_{12} = -(f_n\hat{\mathbf{n}}_1 + f_t\hat{\mathbf{t}}_1 + c_n\mathbf{v}_{12}^{sn} + c_t\mathbf{v}_{12}^{st}), \tag{5}$$

where f_n and f_t are scalar elastic normal and tangential forces and c_n and c_t are normal and tangential damping coefficients.

2.2.1. Normal elastic forces

Overlapping particles ($\delta_n > 0$) are assumed to experience a repulsive normal force of magnitude

$$f_n = K_n\delta_n, \tag{6}$$

where K_n is a normal stiffness. In addition, cohesive particles in close proximity are assumed to attract each other. In this case, Eq. (6) is applied for all $\delta_n > \delta_n^{min} = -K_c\Delta R/(K_n + K_c)$, where K_c is a cohesive stiffness and ΔR is a cut-off distance (Fig. 2). In addition,

$$f_n = -K_c(\delta_n + \Delta R), \tag{7}$$

when $-\Delta R < \delta_n < \delta_n^{min}$. It may be noted that the maximal attractive force has magnitude $f_c = -f_n^{min} = K_nK_c\Delta R/(K_n + K_c)$, and this value may be used to calculate the granular Bond number (Nase et al., 2001) as $Bo_g = f_c/f_g$, where f_g is the magnitude of the force due to gravity.